AIAA JOURNAL
Vol. 39, No. 5, May 2001

Torsional Buckling Analysis of Composite Cylinders

Hoon Cheol Park*
Konkuk University, Seoul 143-701, Republic of Korea
Chahngmin Cho†
Agency for Defense Development, Daejon 305-600, Republic of Korea
and
Younho Choi‡
Korean Aerospace Research Institute, Daejon 305-600, Republic of Korea

A buckling analysis of composite cylinders under torsion is performed by using the geometrically nonlinear finite element analysis. A nine-node assumed strain shell-element model with six degrees of freedom per node is used for the analysis. The buckling load of a composite cylinder is found by searching for a bifurcation point on the geometrically nonlinear deformation path. The corresponding buckling mode is obtained from the eigenvalue analysis at the bifurcation point. Numerical results show good agreement with linear solutions for isotropic and most composite cylinders, but large discrepancies in some cases. This discussion focuses on the pinpoint of the bifurcation point on the nonlinear path and the differences of torsional buckling loads between the nonlinear and linear solutions for various types of composite cylinders.

I. Introduction

A CERTAIN structure can preserve its original shape with very small deformation up to some level of compressive load. This structure experiences abrupt large deformation in a particular pattern after the applied load reaches the so-called buckling load. It is well known that there are two types of buckling: the limit point (snapthrough) and bifurcation. For structures with nonlinear prebuckling behavior, it may be difficult to pinpoint the bifurcation point, whereas tracing the limit point is a relatively easy task.

For a cylinder subjected to torsion, buckling has been predicted by assuming that prebuckling deformation is linear and negligible; in other words, the linear buckling theory. Torsional buckling loads of composite cylinders can be calculated by using shell theories. Tabiei and Simitses[1] used the classical (CL) shell theory that neglects shear deformation of shells and other two shell theories with the first-order shear deformation (FOSD) assumption and higher-order shear deformation (HOSD) assumption to calculate torsional buckling loads of composite cylinders with various radius-to-thickness(R/t) ratios and length-to-radius(L/R) ratios.

Tabiei and Simitses[2] implemented two kinematics assumptions, that is, Donnell-type and Sanders-type assumptions, in their previous shell theories,[1] and they used these theories to estimate torsional buckling loads of moderately thick composite cylinders. In their research, they found that the shell theory based on a Donnell-type assumption provided larger torsional buckling loads than those from the shell theory based on a Sanders-type assumption, as the shell was getting thicker. Therefore, it becomes clear that torsional buckling loads of composite cylinders can be different depending on the kinematics assumptions implemented in the shell theories used for the buckling analysis. Huille et al.[3] computed torsional buckling loads of pipes by using the laminated anisotropic plate theory. Lower buckling loads than Donnell and Flügge's solutions[4] were obtained for thick isotropic cylinders. The paper also provided comparison of their results with experimental buckling loads.

Along with shell theories, the finite element method has been widely used for the buckling analysis of structural members subjected to various external loads. However, papers on the buckling analysis of composite structures under torsion are hard to find in the literature. Nguyen[5] proposed a finite element formulation for the calculation of an accurate torsional constant. Moal et al.[6] formulated a finite element model for the numerical simulation of tension-torsion coupling caused by thermomechanical loading.

Although these studies are based on the linear buckling theory, we need a geometrically nonlinear analysis to obtain the buckling load of a structure when an initial imperfection is imposed on the structure. This is because the imperfection transforms the bifurcation point into a limit point. In contrast, some composite cylinders subjected to torsion, even without imperfections, exhibit geometrically nonlinear behavior from the onset of deformation. In these cases, the torsional buckling problems should be reviewed in terms of a geometrically nonlinear analysis.

The objective of this study is to investigate torsional buckling loads of composite cylinders by using the geometrically nonlinear analysis. For this purpose, the nine-node assumed strain shell-element model[7] is used. Performance of the element in a geometrically nonlinear stability analysis has been proven in previous research.[8] Therefore, detail formulation of the shell element is avoided and only key features are explained. The torsional buckling loads of various composite cylinders are calculated by searching for a bifurcation point on the geometrically nonlinear deformation path without any imperfection. Numerical results are discussed and compared with reference solutions from Tabiei and Simitses[1] and Huille et al.[3]

II. Kinematics of Deformation

Figure 1 represents an enlarged infinitesimal section of the shell. The displacement $\boldsymbol{u}$ at an arbitrary point $\boldsymbol{P}$ can be expressed as follows:

$$\boldsymbol{u} = \boldsymbol{u}_o + \boldsymbol{O'P'} - \boldsymbol{OP} = \boldsymbol{u}_o + \zeta(t/2)(\boldsymbol{a}'_3 - \boldsymbol{a}_3) \tag{1}$$

where $\boldsymbol{u}_o$ is the displacement at the point $\boldsymbol{O}$ lying on the shell midsurface, ζ is the nondimensional coordinate in the thickness direction, and t is the shell thickness. Generally, the degenerated solid shell element neglects deformation in the thickness direction and assumes no thickness change. In this case, the term $(\boldsymbol{a}'_3 - \boldsymbol{a}_3)$ in Eq. (1), which stands for change of the normal vector $\boldsymbol{a}_3$, can be represented with two rotational angles around two in-plane axes. Thus, most shell elements are formulated based on this assumption. Therefore, modeling of thick structures by using the existing shell element may not be appropriate. Moreover, the geometrically nonlinear analyses using those shell elements require large computing times as a result of the inclusion of the two rotation angles as nodal degrees of freedom (DOF).

Received 10 February 2000; revision received 16 June 2000; accepted for publication 29 June 2000.

*Associate Professor, Department of Aerospace Engineering. Member AIAA.
†Senior Researcher.
‡Post-Master Engineer.

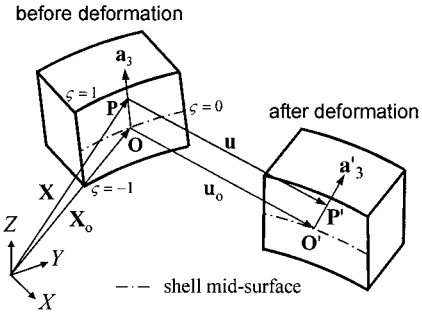

Fig. 1 Kinematics of deformation.

The term $(\boldsymbol{a}_3' - \boldsymbol{a}_3)$ can be represented with one vector that has three components when the thickness is allowed to change. Then, deformation at an arbitrary point is expressed in terms of six DOF, that is, three translational DOF at the point on the shell midsurface and three components of the change of normal vector $(\boldsymbol{a}_3' - \boldsymbol{a}_3)$ as follows:

$$\boldsymbol{u} = \boldsymbol{u}_o + \zeta(t/2)(\boldsymbol{a}_3' - \boldsymbol{a}_3) = \boldsymbol{u}_o + \zeta(t/2)\boldsymbol{u}_z \tag{2}$$

where $\boldsymbol{u}_z = (\boldsymbol{a}_3' - \boldsymbol{a}_3)$. Because the thickness is allowed to change, the shell element may be properly used to model thick shell structures. The present shell element also has merit over the conventional degenerated solid shell elements in the performance of the geometrically nonlinear analysis. Converged solutions can be obtained even for large load increments, because there are no incremental angles in the incremental formulation. At the same time, the shell element is formulated to cope with locking phenomena. These features of the present shell element have been proven in previous studies.[7,8]

III. Computation of Torsioal Buckling Loads

The torsional buckling load of a composite cylinder is obtained by finding the lowest torsion load that makes the determinant of the global tangent stiffness matrix zero in the course of the geometrically nonlinear analysis. The nine-node assumed strain shell element with six DOF per node[7] is used to construct the incremental formulation for the geometrically nonlinear analysis of composite cylinders. Because the detail procedure for the formulation is explained in Ref. 7, we do not duplicate it here.

The Newton–Raphson method is used to obtain converged solutions, and the convergence criteria are as follows:

$$\frac{1}{2}\left(\frac{\|\Delta \boldsymbol{q}_o^{(i)}\|}{\|\boldsymbol{q}_o^{(i-1)}\|} + \frac{\|\Delta \boldsymbol{q}_z^{(i)}\|}{\|\boldsymbol{q}_z^{(i-1)}\|}\right) < \varepsilon \tag{3}$$

where $\Delta \boldsymbol{q}^{(i)}$ is increment of the nodal DOF vector at the current load step, $\boldsymbol{q}^{(i-1)}$ is the nodal DOF vector at the previous load step, and ε is the error permission. In Eq. (3), the subscripts o and z stand for the components of $\boldsymbol{u}_o$ and $\boldsymbol{u}_z$ vectors in Eq. (2), respectively.

As the applied torsion load is increased in the course of the geometrically nonlinear analysis, the determinant of the tangent stiffness matrix is checked if it becomes zero. The lowest torsion load that makes the determinant of the tangent stiffness matrix zero is regarded as the buckling load. The determinant of the tangent stiffness matrix at the current load step $\boldsymbol{K}^{(i)}$ can be expressed as Eq. (4) when the $\boldsymbol{K}^{(i)}$ with n rows and n columns is decomposed as $\boldsymbol{K}^{(i)} = \boldsymbol{L}\boldsymbol{D}\boldsymbol{L}^T$ by using triple factorization. In this case, the determinant of $\boldsymbol{K}^{(i)}$ is expressed as follows:

$$\det \boldsymbol{K}^{(i)} = \prod_{i=1}^{n} \boldsymbol{D}_{ii} \tag{4}$$

where $\boldsymbol{L}$ is the lower triangular matrix and $\boldsymbol{D}$ is the diagonal matrix. Therefore, a composite cylinder subjected to a torsion load become unstable when any one of the diagonal terms $\boldsymbol{D}_{ii}$ is zero.

Because the structural instability can happen for two load types, that is, the limit load and bifurcation load, we need to identify the type of instability. The current stiffness parameter S_p proposed by Bergan et al.[8] is used to distinguish the bifurcation point from the limit point. The current stiffness parameter S_p is expressed as

$$S_p = \frac{\Delta \boldsymbol{q}^{(1)^T} \boldsymbol{P}_o}{\Delta \boldsymbol{q}^{(i)^T} \boldsymbol{P}_o} \tag{5}$$

where $\Delta \boldsymbol{q}^{(1)}$ is the incremental nodal DOF vector at the first load step and $\Delta \boldsymbol{q}^{(i)}$ is the incremental nodal DOF vector at the current load step. The following criteria are used to identify the bifurcation point:

$$\begin{aligned} &\det \boldsymbol{K}^{(i)} = 0, \qquad S_p = 0, \text{ limit point} \\ &\det \boldsymbol{K}^{(i)} = 0, \qquad S_p \neq 0, \text{ bifurcation point} \end{aligned} \tag{6}$$

Increasing the applied torsion load, we may find a torsion load that results in the sign change of $\det \boldsymbol{K}^{(i)}$. When even numbers of instability paths exist, however, the sign of $\det \boldsymbol{K}^{(i)}$ may not be changed and the instability cannot be detected. This situation can be avoided by counting number of negative diagonals of the $\boldsymbol{D}$ matrix in Eq. (4). Buckling load is pinpointed by the bisection iteration between the two torsion loads that make the sign change of $\det \boldsymbol{K}^{(i)}$. The buckling mode for the buckling load is obtained by using the subspace iteration with the Householder and QZ inverse iteration.

IV. Numerical Examples

First, the torsional buckling load of a cylinder made of an isotroptic material is calculated to compare with the linear buckling load and to verify the present approach. Subsequently, composite cylinders with various radius-to-thickness (R/t) ratios and length-to-radius (L/R) ratios are analyzed for the calculation of buckling loads.

Torsional buckling loads of composite cylinders are compared with linear buckling loads from three shell theories. These are the classical shell theory without consideration of shear deformation, shell theories with the FOSD assumption, and those with the HOSD assumption.[1] Comparisons of the present torsional buckling loads of intermediately long composite cylinders with reference solutions from Huille et al.[3] are also provided. Because some of three-dimensional orthotropic material properties such as G_{23} and ν_{23} are not provided in this reference, they are properly assumed according to engineering judgment. In all calculations, the Newton–Raphson method is used to find converged solutions, and the error permission in Eq. (3) is set equal to 10^{-4}.

A. Torsional Buckling Load of an Isotropic Cylinder

Donnell[9] derived the torsional buckling load (τ_{cr}, psi) of the simply supported isotropic cylinder by using the shell theory as Eq. (7) under the assumption of no shear deformation:

$$\tau_{cr} = 2.8\frac{E}{1-\nu^2}\left(\frac{t}{L}\right)^2 + \sqrt{2.6 + 1.40\left(\frac{L^2}{2Rt}\sqrt{1-\nu^2}\right)^{\frac{3}{2}}} \tag{7}$$

where R is the radius, L is the length, t is the thickness of the cylinder, E is Young's modulus, and ν is Poisson's ratio. In the present example, $R = 10$ (in.), $L = 50$ (in.), $t = 0.1$ (in.), $E = 10^7$ (psi), and $\nu = 0.3$. The cylinder geometry, boundary condition, and loading condition are described in Fig. 2.

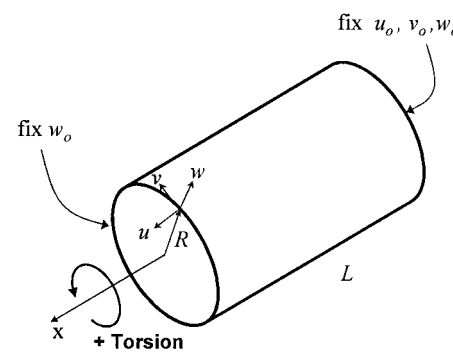

Fig. 2 Simply supported cylinder under torsion.

Table 1 Torsional buckling load of an isotropic cylinder

Mesh	Load, psi	
	Present[a]	Donnell
10×20	10,903 (5, 3.3%)	10,559
15×30	10,735 (6, 1.7%)	

[a](n, p): n is the number of waves in the circumference direction, and p is the relative error.

Table 2 Material properties used in example 1

Property	Value
E_{11}	149.617 GPa
G_{23}	2.551 GPa
ν_{23}	0.45
$E_{22} = E_{33}$	9.928 GPa
$G_{12} = G_{13}$	4.481 GPa
$\nu_{12} = \nu_{13}$	0.28

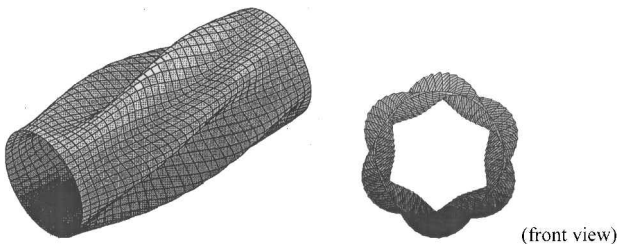

Fig. 3 Torsional buckling mode of an isotropic cylinder.

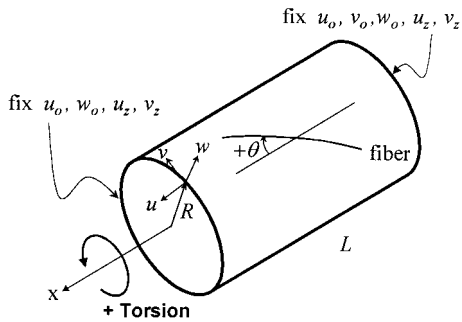

Fig. 4 Fixed composite cylinder under torsion.

The results of the calculation are summarized in Table 1. With the 15×30 mesh (15 and 30 elements in the longitudinal direction and in the circumference directions, respectively), the present analysis using the nine-node geometrically nonlinear assumed strain shell element has computed a converged solution very close to Donnell's solution.[9] The buckling mode of the buckled cylinder is shown in Fig. 3.

B. Torsional Buckling of Composite Cylinders

Example 1

Tabiei and Simitses[1] reported linear torsional buckling loads of composite cylinders with various R/t ratios and L/R ratios. In the present example, composite cylinders with $R = 0.1905$ m, $R/L = 1$ or 5, $R/t = 15$ or 100, and ply orientations $[0/90/0]_s$, $[30/30/-60]_s$, and $[-45/-45/45]_s$ are analyzed to calculate torsional buckling loads. Positive ply angle and positive torsion load are described in Fig. 4. Material properties used for the analysis are summarized in Table 2 (Ref. 1).

It has been found that the finite element model with a refined mesh in the circumference direction shows better convergence than with the refined model in the logitudianl direction. In the present example, therefore, we used 8×40 meshes for composite cylinders with $L/R = 1$, and 16×40 meshes for those with $L/R = 5$, regardless of R/t. When the obtained buckling mode of a composite cylinder coincides with that from a reference solution, then the computed buckling load becomes insensitive to the mesh refinement. Numerical results from the present approach are compared with the reference linear buckling loads[1] in Tables 3–6.

Table 3 Torsional buckling loads: $R/t = 100$ and $[0/90/0]_s$

L/R	Load, $\times 10^6$ N/m	
	Present	Tabiei and Simitses[a]
1	0.1714 (9)	CL, 0.1576 (9)
		FOSD, 0.1568 (9)
		HOSD, 0.1559 (9)
5	0.0806 (6)	CL, 0.0757 (6)
		FOSD, 0.0757 (6)
		HOSD, 0.0757 (6)

[a](n): n is the number of waves in the circumference direction.

Table 4 Torsional buckling loads: $R/t = 15$ and $[0/90/0]_s$

L/R	Load, $\times 10^6$ N/m	
	Present	Tabiei and Simitses[a]
1	NA	CL, 29.320 (5)
		FOSD, 17.822 (5)
		HOSD, 16.499 (6)
5	NA	CL, 4.2910 (3)
		FOSD, 4.1510 (3)
		HOSD, 4.0985 (3)

[a](n): n is the number of waves in the circumference direction.

Table 5 Torsional buckling loads: $R/t = 100$ and $[30/30/-60]_s$

L/R	Load, $\times 10^6$ N/m	
	Present	Tabiei and Simitses[a]
1	0.2160 (9)	CL, 0.3030 (9)
		FOSD, 0.2978 (9)
		HOSD, 0.2934 (9)
5	0.0544 (5)	CL, 0.0613 (5)
		FOSD, 0.0613 (5)
		HOSD, 0.0613 (5)

[a](n): n is the number of waves in the circumference direction.

Table 6 Torsional buckling loads: $R/t = 15$ and $[30/30/-60]_s$

L/R	Load, $\times 10^6$ N/m	
	Present	Tabiei and Simitses[a]
1	14.840 (5)	CL, 56.048 (5)
		FOSD, 27.218 (6)
		HOSD, 23.855 (6)
5	4.5256 (3)	CL, 6.1920 (3)
		FOSD, 5.6398 (3)
		HOSD, 5.4820 (3)

[a](n): n is the number of waves in the circumference direction.

Table 3 summarizes torsional buckling loads of thin composite cylinders with $R/t = 100$ and $[0/90/0]_s$. Because thicknesses of the cylinders are thin, reference solutions from three shell theories with different assumptions of shear deformation[1] are almost identical to each other. Torsional buckling loads from the present method are slightly different from these reference solutions. The present buckling loads of the short cylinder ($L/R = 1$) and the long cylinder ($L/R = 5$) are 9.3 and 6.5% larger than those from the linear buckling analyses (FOSD),[1] respectively. The buckling modes coincide with reference solutions for the two cases. Figure 5 shows the buckling mode of the composite cylinder ($R/t = 100, L/R = 1$) with $[0/90/0]_s$.

Torsional buckling loads of thick composite cylinders with $R/t = 15$ and $[0/90/0]_s$ are summarized in Table 4. In both cases of composite cylinders with $L/R = 1$ and 5, the torsion loads that

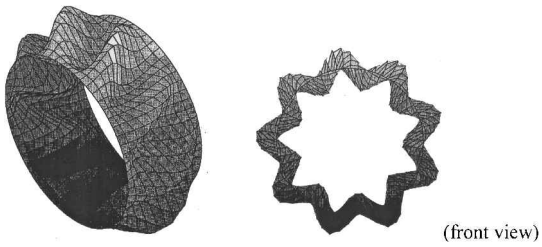

Fig. 5 Buckling mode: $R/t = 100$, $L/R = 1$, $[0/90/0]_s$.

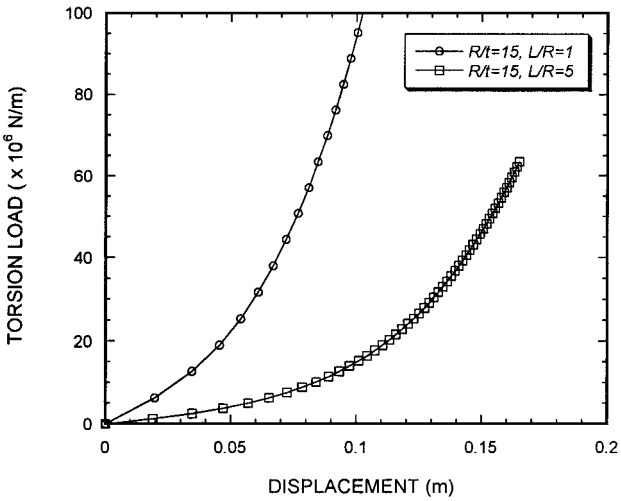

Fig. 6 Stiffening of thick composite cylinders with $R/t = 15$ and $[0/90/0]_s$.

make $\det \boldsymbol{K}^{(i)} = 0$ could not be found, because the determinant of the tangent stiffness matrix grew up without a sign change. Figure 6 shows the stiffening for the two cylinders. However, the linear buckling analysis using the shell theories[1] provides torsional buckling loads.

Table 5 summarizes torsional buckling loads of thin composite cylinders with $R/t = 100$ and $[30/30/-60]_s$. Because the cylinders are thin again, reference solutions from three different shell theories[1] are almost identical. The present buckling loads of the short cylinder ($L/R = 1$) and the long cylinder ($L/R = 5$) are 27 and 11% smaller than those from the linear buckling analyses (FOSD),[1] respectively. Buckling modes coincide with reference solutions for the two cases.

Torsional buckling loads of thick composite cylinders ($R/t = 15$) with $[30/30/-60]_s$ are compared with reference solutions[1] in Table 6. In this case, the stiffening is not observed other than in the previous thick composite cylinder ($R/t = 15$) with $[0/90/0]_s$. Torsional buckling load of a short cylinder ($L/R = 1$) is 45% less and that of a long cylinder ($L/R = 5$) is 20% less than reference linear buckling loads (FOSD). The buckling mode of the short cylinder coincides with the mode obtained from the classical shell theory, and the mode of the long cylinder is identical to the one from the linear buckling analysis using the shell theories.

For thin composite cylinders ($R/t = 100$) with $[-45/-45/45]_s$, buckling modes are slightly different from those obtained by using the linear buckling analyses as summarized in Table 7. However, the present buckling loads for the two cylinders are very close to the reference solutions. The buckling load of the short cylinder is 4.9% larger and that of the long one is 2.7% larger than the reference solutions (FOSD).

In Table 8, torsional buckling loads of thick composite cylinders ($R/t = 15$) with $[-45/-45/45]_s$ are compared with reference solutions. The present buckling loads are 1.9–1.0% larger than linear buckling loads (FOSD) for the short and long cylinders. Buckling modes of the two composite cylinders agree well with the reference solutions.

Comparing the present results and the reference linear buckling loads[1] based on the shell theories, we can summarize the results as follows:

Table 7 Torsional buckling loads: $R/t = 100$ and $[-45/-45/45]_s$

	Load, $\times 10^6$ N/m	
L/R	Present[a]	Tabiei and Simitses[a]
1	0.1448 (13)	CL, 0.1419 (14)
		FOSD, 0.1410 (14)
		HOSD, 0.1401 (14)
5	0.0511 (6)	CL, 0.0497 (7)
		FOSD, 0.0487 (7)
		HOSD, 0.0497 (7)

[a] (n): n is the number of waves in the circumference direction.

Table 8 Torsional buckling loads: $R/t = 15$ and $[-45/-45/45]_s$

	Load, $\times 10^6$ N/m	
L/R	Present[a]	Tabiei and Simitses[a]
1	11.028 (7)	CL, 13.486 (7)
		FOSD, 11.244 (7)
		HOSD, 10.851 (7)
5	3.7154 (4)	CL, 3.7306 (4)
		FOSD, 3.6782 (4)
		HOSD, 3.6519 (4)

[a] (n): n is the number of waves in the circumference direction.

Table 9 Material properties of Br/Epoxy AVCO 5505/4[a]

Property	Value
E_{11}	218 GPa
G_{23}	G_{12}^{b}
ν_{23}	0.42[b]
$E_{22} = E_{33}$	18.6 GPa
$G_{12} = G_{13}$	6.89 GPa
$\nu_{12} = \nu_{13}$	0.21

[a] From Ref. 10. [b] Assumed material properties.

1) Buckling modes from the two analyses agree well with each other for most cases. For the thin composite cylinders with $[-45/-45/45]_s$, the present buckling modes are slightly different from those obtained by using the linear buckling analyses.

2) The present method cannot find the bifurcation point of thick composite cylinders ($R/t = 15$) with $[0/90/0]_s$ as a result of stiffening. For thin cylinders ($R/t = 100$) with $[0/90/0]_s$, buckling loads are close to the linear buckling loads.

3) For composite cylinders with $[30/30/-60]_s$, the present torsional buckling loads are 11–45% less than the linear buckling loads from the shell theories.

4) Torsional buckling loads of composite cylinders with $[-45/-45/45]_s$ are close to the linear buckling loads based on the shell theories.

Example 2

Huille et al.[3] computed linear buckling loads of relatively long composite cylinders (pipes) by using the anisotropic laminated plate theory and the Ritz method. They compared their results with experimental results obtained by Herakovich and Johnson[10] and torsional buckling loads calculated by Wu[11] based on the nonlinear equilibrium equation. In the present example, the torsional buckling loads of three composite cylinders are compared with reference solutions.[3] The three composite cylinder have the following specifications: cylinder 1, $[0]_8$, $R = 0.07536$ m, $L = 0.3556$ m, $t = 0.00094232$ m ($R/t = 80$, $L/R = 4.7$); and cylinders 2 and 3, $[0/45/-45/90]_s$ or $[0/-45/45/-90]_s$, $R = 0.07562$ m, $L = 0.4826$ m, $t = 0.00096528$ m ($R/t = 78$, $L/R = 6.4$).

Material properties used in the computation are listed in Table 9. The properties that are not provided in Ref. 3 are properly assumed to construct the three-dimensional orthotropic constitutive law. The

Table 10 Torsional buckling loads of composite cylinders

Ply orientation	Load,[a] N-m			
	Present	Wu[11]	Huill[3]	Herakovich[10]
$[0]_8$	1427 (+41.5%)	1550 (+53.5%)	1360 (+34.7%)	1010
$[0/\pm 45/90]_s$	2698 (+3.4%)	2640 (−1.9%)	2432 (−9.6%)	2690
$[0/-45/45/-90]_s$	2388 (+1.6%)	2240 (−4.7%)	2026 (−13.8%)	2350

[a](%): relative error; the experimental data from Ref. 10 are taken as a reference.

three composite cylinders are modeled by using the 14×36 mesh. Two ends of the cylinders are fixed, so that experiments done by Herakovich and Johnson[10] can be simulated.

In Table 10, the computed torsional buckling loads of the composite cylinders are compared with the three reference solutions.[3] Relative errors to the Harakovich's experimental data[10] are given in parentheses. For composite cylinders with $[0/45/-45/90]_s$ and $[0/-45/45/-90]_s$, especially, the present solutions agree well with the experimental data[10] as well as analytical solutions from Wu.[11] Note that the present buckling loads agree better with the experimental data[10] than Huille's linear buckling loads[3] do. For composite cylinders with $[0]_8$, however, all of three numerical results show large discrepancies with the experimental data. Because the composite cylinder with $[0]_8$ is sensitive to the initial geometric imperfection, unlike composite cylinders with angle plies, the composite cylinder with $[0]_8$ may have buckled prematurely during the experiment.

V. Conclusions

In the present paper, torsional buckling loads of various composite cylinders have been calculated by using the geometrically nonlinear assumed strain shell element. The critical torsion load is pinpointed by checking the determinant of the global stiffness matrix as the applied load is increased. The load parameter is used to distinguish the bifurcation point from the limit point. When the determinant of the global tangent stiffness matrix becomes zero and the load parameter is not zero for a certain load step, the load size is regarded as the bifurcation load.

Buckling modes of most composite cylinders obtained from the present method agree well with the modes from reference solutions based on the linear buckling analysis, regardless of the ply orientation, the thickness, and the length of cylinders. As for buckling loads, no simple tendency can be found. Torsional buckling loads are close to the linear buckling loads only for thin composite cylinders ($R/t = 100$) with $[45/45/-45]_s$ ply orientation. Up to 45% lower buckling loads than the linear buckling loads are computed for composite cylinders with $[30/30/-60]_s$. For thick composite cylinders ($R/t = 15$) with $[0/90/0]_s$, no critical point can be found because of the stiffening.

Therefore, it is found that torsional buckling loads calculated by the present method can show a large discrepancy with the linear buckling loads, depending on the ply orientation of composite cylinders. Comparing the present torsional buckling of moderately long composite cylinders with experimental data, we have confirmed that the present method can more accurately predict torsional buckling loads of composite cylinders than the other linear buckling analyses. The present method can be used to find buckling loads of geometrically imperfect composite cylinders.

Acknowledgment

This work was supported by grant 981-1003-018-1 from the Basic Research program of the KOSEF. The authors thank KOSEF for supporting the present research.

References

[1]Tabiei, A., and Simitses, G., "Buckling of Moderately Thick, Laminated Cylindrical Shells Under Torsion," *AIAA Journal*, Vol. 32, No. 3, 1994, pp. 639–647.

[2]Tabiei, A., and Simitses, G., "Torsional Instability of Moderately Thick Composite Cylindrical Shells by Various Shell Theories," *AIAA Journal*, Vol. 37, No. 7, 1997, pp. 1243–1246.

[3]Huille, A., Tang, C., and Pang, S., "Buckling Analysis of Thick-Walled Composite Pipe Under Torsion," *Journal of Pressure Vessel Technology*, Vol. 119, No. 1, 1997, pp. 111–121.

[4]Timoshenko, S. P., and Gere, J. M., *Theory of Elastic Stability*, 3rd ed., McGraw–Hill, New York, 1963, pp. 500–509.

[5]Nguyen, S. H., "An Accurate Finite Element Formulation for Linear Elastic Torsion Calculations," *Computers and Structures*, Vol. 42, No. 5, 1992, pp. 707–711.

[6]Moal, A., Massoni, E., and Chenot, J. L., "A Finite Element Model for Simulation of the Torsion and Torsion-Tension Tests," *Computer Methods in Applied Mechanics and Engineering*, Vol. 103, No. 3, 1986, pp. 417–425.

[7]Park, H. C., Cho, C., and Lee, S. W., "An Efficient Assumed Strain Element Model with Six DOF Per Node for Geometrically Non-Linear Shell," *International Journal of Numerical Method in Engineering*, Vol. 38, No. 24, 1995, pp. 4101–4122.

[8]Cho, C., Park, H. C., and Lee, S. W., "Stability Analysis Using a Geometrically Nonlinear Assumed Strain Solid Shell Element Model," *Finite Elements in Analysis and Design*, Vol. 29, No. 2, 1998, pp. 121–135.

[9]Bergan, P. G., et al., "Solution Techniques for Nonlinear Finite Element Problems," *International Journal for Numerical Method in Engineering*, Vol. 12, 1978, pp. 1677–1696.

[10]Herakovich, C. T., and Johnson, E. R., "Buckling of Composite Cylinders Under Combined Compression and Torsion-Theoretical/Experimental Correlation," *Test Methods and Design Allowables for Fibrous Composites*, ASTM STP 734, edited by C. C. Chamis, American Society for Testing Materials, Philadelphia, PA, 1981, pp. 341–360.

[11]Wu, C. H., "Buckling of Anisotropic Circular Shells," Ph.D. Dissertation, Case Western Reserve Univ., Cleveland, OH, 1971.

A. N. Palazotto
Associate Editor